Control of dynamical systems via time-delayed feedback and unstable controller

K. Pyragas*

Semiconductor Physics Institute and Vilnius Pedagogical University, Vilnius, Lithuania

(Dated: January 28, 2003)

Abstract

Time delayed-feedback control is an efficient method for stabilizing unstable periodic orbits of chaotic systems. The method is based on applying feedback proportional to the deviation of the current state of the system from its state one period in the past so that the control signal vanishes when the stabilization of the desired orbit is attained. A brief review of experimental implementations, applications for theoretical models, and most important modifications of the method is presented. Some recent results concerning the theory of the delayed feedback control as well as an idea of using unstable degrees of freedom in a feedback loop to avoid a well known topological limitation of the method are described in details.

*Electronic address: pyragas@kes0.pfi.lt

I. INTRODUCTION

Control of dynamical systems is a classical subject in engineering science [1, 2]. The revived interest of physicists in this subject started with an idea of controlling chaos [3]. Wy chaotic systems are interesting objects for control theory and applications? The major key ingredient for the control of chaos is the observation that a chaotic set, on which the trajectory of the chaotic process lives, has embedded within it a large number of unstable periodic orbits (UPOs). In addition, because of ergodicity, the trajectory visits or accesses the neighborhood of each one of these periodic orbits. Some of these periodic orbits may correspond to a desired system's performance according to some criterion. The second ingredient is the realization that chaos, while signifying sensitive dependence on small changes to the current state and henceforth rendering unpredictable the system state in the long time, also implies that the system's behavior can be altered by using small perturbations. Then the accessibility of the chaotic system to many different period orbits combined with its sensitivity to small perturbations allows for the control and manipulation of the chaotic process. These ideas stimulated a development of rich variety of new chaos control techniques (see Ref. [4] for review), among which the delayed feedback control (DFC) method [5] has gained widespread acceptance.

The DFC method is based on applying feedback proportional to the deviation of the current state of the system from its state one period in the past so that the control signal vanishes when the stabilization of the desired orbit is attained. Alternatively the DFC method is referred to as a method of time-delay autosynchronization, since the stabilization of the desired orbit manifests itself as a synchronization of the current state of the system with its delayed state. The DFC has the advantage of not requiring prior knowledge of anything but the period of the desired orbit. It is particularly convenient for fast dynamical systems since does not require the real-time computer processing. Experimental implementations, applications for theoretical models, and most important modifications of the DFC method are briefly listed below.

Experimental implementations.— The time-delayed feedback control has been successfully used in quite diverse experimental contexts including electronic chaos oscillators [6], mechanical pendulums [7], lasers [8], a gas discharge system [9, 10], a current-driven ion acoustic instability [11], a chaotic Taylor-Couette flow [12], chemical systems [13], high-

power ferromagnetic resonance [14], helicopter rotor blades [15], and a cardiac system [16].

Applications for theoretical models.— The DFC method has been verified for a large number of theoretical models from different fields. Simmendinger and Hess [17] proposed an all-optical scheme based on the DFC for controlling delay-induced chaotic behavior of high-speed semiconductor lasers. The problem of stabilizing semiconductor laser arrays has been considered as well [18]. Rappel, Fenton, and Karma [19] used the DFC for stabilization of spiral waves in an excitable media as a model of cardiac tissue in order to prevent the spiral wave breakup. Konishi, Kokame, and Hirata [20] applied the DFC in a model of a car-following traffic. Batlle, Fossas, and Olivar [21] implemented the DFC in a model of buck converter. Bleich and Socolar [22] showed that the DFC can stabilize regular behavior in a paced, excitable oscillator described by Fitzhugh-Nagumo equations. Holyst, Zebrowska, and Urbanowicz [23] used the DFC to control chaos in economical model. Tsui and Jones investigated the problem of chaotic satellite attitude control [24] and constructed a feedforward neural network with the DFC to demonstarte a retrieval behavior that is analogous to the act of recognition [25]. The problem of controlling chaotic solitons by a time-delayed feedback mechanism has been considered by Fronczak and Holyst [26]. Mensour and Longtin [27] proposed to use the DFC in order to store information in delay-differential equations. Galvanetto [28] demonstrated the delayed feedback control of chaotic systems with dry friction. Lastly, Mitsubori and Aihara [29] proposed rather exotic application of the DFC, namely, the control of chaotic roll motion of a flooded ship in waves.

Modifications.—A reach variety of modifications of the DFC have been suggested in order to improve its performance. Adaptive versions of the DFC with automatic adjustment of delay time [30] and control gain [31] have been considered. Basso *et al.* [32] showed that for a Lur'e system (system represented as feedback connection of a linear dynamical part and a static nonlinearity) the DFC can be optimized by introducing into a feedback loop a linear filter with an appropriate transfer function. For spatially extended systems, various modifications based on spatially filtered signals have been considered [33]. The wave character of dynamics in some systems allows a simplification of the DFC algorithm by replacing the delay line with the spatially distributed detectors. Mausbach *et al.* [10] reported such a simplification for a ionization wave experiment in a conventional cold cathode glow discharge tube. Due to dispersion relations the delay in time is equivalent to the spatial displacement and the control signal can be constructed without use of the delay

line. Socolar, Sukow, and Gauthier [34] improved an original DFC scheme by using an information from many previous states of the system. This extended DFC (EDFC) scheme achieves stabilization of UPOs with a greater degree of instability [35, 36]. The EDFC presumably is the most important modification of the DFC and it will be discussed at greater length in this paper.

The theory of the DFC is rather intricate since it involves nonlinear delay-differential equations. Even linear stability analysis of the delayed feedback systems is difficult. Some general analytical results have been obtained only recently [37–40]. It has been shown that the DFC can stabilize only a certain class of periodic orbits characterized by a finite torsion. More precisely, the limitation is that any UPOs with an odd number of real Floquet multipliers (FMs) greater than unity (or with an odd number of real positive Floquet exponents (FEs)) can never be stabilized by the DFC. This statement was first proved by Ushio [37] for discrete time systems. Just *et al.* [38] and Nakajima [39] proved the same limitation for the continuous time DFC, and then this proof was extended for a wider class of delayed feedback schemes, including the EDFC [40]. Hence it seems hard to overcome this inherent limitation. Two efforts based on an oscillating feedback [41] and a half-period delay [42] have been taken to obviate this drawback. In both cases the mechanism of stabilization is rather unclear. Besides, the method of Ref. [42] is valid only for a special case of symmetric orbits. The limitation has been recently eliminated in a new modification of the DFC that does not utilize the symmetry of UPOs [43]. The key idea is to introduce into a feedback loop an additional unstable degree of freedom that changes the total number of unstable torsion-free modes to an even number. Then the idea of using unstable degrees of freedom in a feedback loop was drown on to construct a simple adaptive controller for stabilizing unknown steady states of dynamical systems [44].

Some recent theoretical results on the DFC method and the unstable controller are presented in more details in the rest of the paper. Section II is devoted to the theory of the DFC. We show that the main stability properties of the system controlled by time-delayed feedback can be simply derived from a leading Floquet exponent defining the system behavior under proportional feedback control (PFC). We consider the EDFC versus the PFC and derive the transcendental equation relating the Floquet spectra of these two control methods. At first we suppose that the FE for the PFC depends linearly on the control gain and derive the main stability properties of the EDFC. Then the case of nonlinear dependence is

considered for the specific examples of the Rössler and Duffing systems. For these examples we discuss the problem of optimizing the parameters of the delayed feedback controller. In Section III the problem of stabilizing torsion-free periodic orbits is considered. We start with a simple discrete time model and show that an unstable degree of freedom introduced into a feedback loop can overcome the limitation of the DFC method. Then we propose a generalized modification of the DFC for torsion-free UPOs and demonstrate its efficiency for the Lorenz system. Section IV is devoted to the problem of adaptive stabilization of unknown steady states of dynamical systems. We propose an adaptive controller described by ordinary differential equations and prove that the steady state can never be stabilized if the system and controller in sum have an odd number of real positive eigenvalues. We show that the adaptive stabilization of saddle-type steady states requires the presence of an unstable degree of freedom in a feedback loop. The paper is finished with conclusions presented in Section V.

II. THEORY OF TIME-DELAYED FEEDBACK CONTROL

If the equations governing the system dynamics are known the success of the DFC method can be predicted by a linear stability analysis of the desired orbit. Unfortunately, usual procedures for evaluating the Floquet exponents of such systems are rather intricate. Here we show that the main stability properties of the system controlled by time-delayed feedback can be simply derived from a leading Floquet exponent defining the system behavior under proportional feedback control [45]. As a result the optimal parameters of the delayed feedback controller can be evaluated without an explicit integration of delay-differential equations.

Several numerical methods for the linear stability analysis of time-delayed feedback systems have been developed. The main difficulty of this analysis is related to the fact that periodic solutions of such systems have an infinite number of FEs, though only several FEs with the largest real parts are relevant for stability properties. Most straightforward method for evaluating several largest FEs is described in Ref. [35]. It adapts the usual procedure of estimating the Lyapunov exponents of strange attractors [46]. This method requires a numerical integration of the variational system of delay-differential equations. Bleich and Socolar [36] devised an elegant method to obtain the stability domain of the system under EDFC in which the delay terms in variational equations are eliminated due to the Floquet

theorem and the explicit integration of time-delay equations is avoided. Unfortunately, this method does not define the values of the FEs inside the stability domain and is unsuitable for optimization problems.

An approximate analytical method for estimating the FEs of time-delayed feedback systems has been developed in Refs. [38, 47]. Here as well as in Ref. [36] the delay terms in variational equations are eliminated and the Floquet problem is reduced to the system of ordinary differential equations. However, the FEs of the reduced system depend on a parameter that is a function of the unknown FEs itself. In Refs. [38, 47] the problem is solved on the assumption that the FE of the reduced system depends linearly on the parameter. This method gives a better insight into mechanism of the DFC and leads to reasonable qualitative results. Here we use a similar approach but do not employ the above linear approximation and show how to obtain the exact results. In this section we do not consider the problem of stabilizing torsion-free orbits and restrict ourselves to the UPOs that are originated from a flip bifurcation.

A. Proportional versus time-delayed feedback

Consider a dynamical system described by ordinary differential equations

$$\dot{\boldsymbol{x}} = \boldsymbol{f}(\boldsymbol{x}, p, t), \tag{1}$$

where the vector $\boldsymbol{x} \in R^m$ defines the dynamical variables and p is a scalar parameter available for an external adjustment. We imagine that a scalar variable

$$y(t) = g\big(\boldsymbol{x}(t)\big) \tag{2}$$

that is a function of dynamic variables $\boldsymbol{x}(t)$ can be measured as the system output. Let us suppose that at $p = 0$ the system has an UPO $\boldsymbol{x}_0(t)$ that satisfies $\dot{\boldsymbol{x}}_0 = \boldsymbol{f}(\boldsymbol{x}_0, 0, t)$ and $\boldsymbol{x}_0(t + T) = \boldsymbol{x}_0(t)$, where T is the period of the UPO. Here the value of the parameter p is fixed to zero without a loss of generality. To stabilize the UPO we consider two continuous time feedback techniques, the PFC and the DFC, both introduced in Ref. [5].

The PFC uses the periodic reference signal

$$y_0(t) = g\big(\boldsymbol{x}_0(t)\big) \tag{3}$$

that corresponds to the system output if it would move along the desired UPO. For chaotic systems, this periodic signal can be reconstructed [5] from the chaotic output $y(t)$ by using the standard methods for extracting UPOs from chaotic time series data [48]. The control is achieved via adjusting the system parameter by a proportional feedback

$$p(t) = G\left[y_0(t) - y(t)\right], \tag{4}$$

where G is the control gain. If the stabilization is successful the feedback perturbation $p(t)$ vanishes. The experimental implementation of this method is difficult since it is not simply to reconstruct the UPO from experimental data.

More convenient for experimental implementation is the DFC method, which can be derived from the PFC by replacing the periodic reference signal $y_0(t)$ with the delayed output signal $y(t-T)$ [5]:

$$p(t) = K\left[y(t-T) - y(t)\right]. \tag{5}$$

Here we exchanged the notation of the feedback gain for K to differ it from that of the proportional feedback. The delayed feedback perturbation (5) also vanishes provided the desired UPO is stabilized. The DFC uses the delayed output $y(t-T)$ as the reference signal and the necessity of the UPO reconstruction is avoided. This feature determines the main advantage of the DFC over the PFC.

Hereafter, we consider a more general (extended) version of the delayed feedback control, the EDFC, in which a sum of states at integer multiples in the past is used [34]:

$$p(t) = K\left[(1-R)\sum_{n=1}^{\infty} R^{n-1} y(t-nT) - y(t)\right]. \tag{6}$$

The sum represents a geometric series with the parameter $|R| < 1$ that determines the relative importance of past differences. For $R = 0$ the EDFC transforms to the original DFC. The extended method is superior to the original in that it can stabilize UPOs of higher periods and with larger FEs. For experimental implementation, it is important that the infinite sum in Eq. (6) can be generated using only single time-delay element in the feedback loop.

The success of the above methods can be predicted by a linear stability analysis of the desired orbit. For the PFC method, the small deviations from the UPO $\delta\boldsymbol{x}(t) = \boldsymbol{x}(t) - \boldsymbol{x}_0(t)$ are described by variational equation

$$\delta\dot{\boldsymbol{x}} = \left[A(t) + GB(t)\right]\delta\boldsymbol{x}, \tag{7}$$

where $A(t) = A(t+T)$ and $B(t) = B(t+T)$ are both T - periodic $m \times m$ matrices

$$A(t) \;=\; D_1 \boldsymbol{f}\big(\boldsymbol{x}_0(t), 0, t\big), \tag{8a}$$

$$B(t) \;=\; D_2 \boldsymbol{f}\big(\boldsymbol{x}_0(t), 0, t\big) \otimes Dg\big(\boldsymbol{x}_0(t)\big). \tag{8b}$$

Here D_1 (D_2) denotes the vector (scalar) derivative with respect to the first (second) argument. The matrix $A(t)$ defines the stability properties of the UPO of the free system and $B(t)$ is the control matrix that contains all the details on the coupling of the control force.

Solutions of Eq. (7) can be decomposed into eigenfunctions according to the Floquet theory,

$$\delta\boldsymbol{x} = \exp(\Lambda t)\boldsymbol{u}(t), \quad \boldsymbol{u}(t) = \boldsymbol{u}(t+T), \tag{9}$$

where Λ is the FE. The spectrum of the FEs can be obtained with the help of the fundamental $m \times m$ matrix $\Phi(G,t)$ that is defined by equalities

$$\dot{\Phi}(G,t) = \left[A(t) + GB(t)\right]\Phi(G,t), \quad \Phi(G,0) = I. \tag{10}$$

For any initial condition $\boldsymbol{x}_{in}$, the solution of Eq. (7) can be expressed with this matrix, $\boldsymbol{x}(t) = \Phi(G,t)\boldsymbol{x}_{in}$. Combining this equality with Eq. (9) one obtains the system $\left[\Phi(G,T) - \exp(\Lambda T)I\right]\boldsymbol{x}_{in} = 0$ that yields the desired eigensolutions. The characteristic equation for the FEs reads

$$\det\left[\Phi(G,T) - \exp(\Lambda T)I\right] = 0. \tag{11}$$

It defines m FEs Λ_j (or Floquet multipliers $\mu_j = \exp(\Lambda_j T)$), $j = 1 \ldots m$ that are the functions of the control gain G:

$$\Lambda_j = F_j(G), \quad j = 1, \ldots, m. \tag{12}$$

The values $F_j(0)$ are the FEs of the free system. By assumption, at least one FE of the free UPO has a positive real part. The PFC is successful if the real parts of all eigenvalues are negative, $\mathrm{Re}F_j(G) < 0$, $j = 1, \ldots, m$ in some interval of the parameter G.

Consider next the stability problem for the EDFC. The variational equation in this case reads

$$\begin{aligned} \delta\dot{\boldsymbol{x}} \;=\; & A(t)\delta\boldsymbol{x}(t) + KB(t) \\ & \times \left[(1-R)\sum_{n=1}^{\infty} R^{n-1}\delta\boldsymbol{x}(t-nT) - \delta\boldsymbol{x}(t)\right]. \end{aligned} \tag{13}$$

The delay terms can be eliminated due to Eq. (9), $\delta\boldsymbol{x}(t-nT) = \exp(-n\Lambda T)\delta\boldsymbol{x}(t)$. As a result the problem reduces to the system of ordinary differential equations similar to Eq. (7)

$$\delta\dot{\boldsymbol{x}} = [A(t) + KH(\Lambda)B(t)]\,\delta\boldsymbol{x}, \tag{14}$$

where

$$H(\Lambda) = \frac{1-\exp(-\Lambda T)}{1-R\exp(-\Lambda T)} \tag{15}$$

is the transfer function of the extended delayed feedback controller. Eqs. (7) and (14) have the same structure defined by the matrices $A(t)$ and B(t) and differ only by the value of the control gain. The equations become identical if we substitute $G = KH(\Lambda)$. The price one has to pay for the elimination of the delay terms is that the characteristic equation defining the FEs of the EDFC depends on the FEs itself:

$$\det\left[\Phi\big(KH(\Lambda), T\big) - \exp(\Lambda T)I\right] = 0. \tag{16}$$

Nevertheless, we can take advantage of the linear stability analysis for the PFC in order to predict the stability of the system controlled by time-delayed feedback. Suppose, that the functions $F_j(G)$ defining the FEs for the PFC are known. Then the FEs of the UPO controlled by time-delayed feedback can be obtained through solution of the transcendental equations

$$\Lambda = F_j\big(KH(\Lambda)\big), \quad j = 1\ldots m. \tag{17}$$

Though a similar reduction of the EDFC variational equation has been considered previously (cf. Refs. [36, 38, 47]) here we emphasize the physical meaning of the functions $F_j(G)$, namely, these functions describe the dependence of the Floquet exponents on the control gain in the case of the PFC.

In the general case the analysis of the transcendental equations (17) is not a simple task due to several reasons. First, the analytical expressions of the functions $F_j(G)$ are usually unknown; they can be evaluated only numerically. Second, each FE of the free system $F_j(0)$ yields an infinite number of distinct FEs at $K \neq 0$; different eigenvalue branches that originate from different exponents of the free system may hibridizate or cross so that the branches originating from initially stable FEs may become dominant in some intervals of the parameter K [47]. Third, the functions F_j in the proportional feedback technique are defined for the real-valued argument G, however, we may need a knowledge of these functions for the complex values of the argument $KH(\Lambda)$ when considering the solutions of Eqs. (17).

In spite of the above difficulties that may emerge generally there are many specific, practically important problems, for which the most important information on the EDFC performance can be simply extracted from Eqs. (15) and (17). Such problems cover low dimensional systems whose UPOs arise from a period doubling bifurcation.

In what follows we concentrate on special type of free orbits, namely, those that flip their neighborhood during one turn. More specifically, we consider UPOs whose leading Floquet multiplier is real and negative so that the corresponding FE obeys $\mathrm{Im}F_1(0) = \pi/T$. It means that the FE is placed on the boundary of the "Brillouin zone." Such FEs are likely to remain on the boundary under various perturbations and hence the condition $\mathrm{Im}F_1(G) = \pi/T$ holds in some finite interval of the control gain $G \in [G_{min}, G_{max}]$, $G_{min} < 0$, $G_{max} > 0$. Subsequently we shall see that the main properties of the EDFC can be extracted from the function $\mathrm{Re}F_1(G)$, with the argument G varying in the above interval.

Let us introduce the dimensionless function

$$\phi(G) = F_1(G)T - i\pi \tag{18}$$

that describes the dependence of the real part of the leading FE on the control gain G for the PFC and denote by

$$\lambda = \Lambda T - i\pi \tag{19}$$

the dimensionless FE of the EDFC shifted by the amount π along the complex axes. Then from Eqs. (15) and (17) we derive

$$\lambda = \phi(G), \tag{20a}$$

$$K = G\frac{1 + R\exp\big(-\phi(G)\big)}{1 + \exp\big(-\phi(G)\big)}. \tag{20b}$$

These equations define the parametric dependence λ versus K for the EDFC. Here G is treated as an independent real-valued parameter. We suppose that it varies in the interval $[G_{min}, G_{max}]$ so that the leading exponent $F_1(G)$ associated with the PFC remains on the boundary of the "Brillouin zone." Then the variables λ, K, and the function ϕ are all real-valued.

To demonstrate the benefit of Eqs. (20) let us derive the stability threshold of the UPO controlled by the extended time-delayed feedback. The stability of the periodic orbit is changed when λ reverses the sign. From Eq. (20a) it follows that the function $\phi(G)$ has

to vanish for some value $G = G_1$, $\phi(G_1) = 0$. The value of the control gain G_1 is nothing but the stability threshold of the UPO controlled by the proportional feedback. Then from Eq. (20b) one obtains the stability threshold

$$K_1 = G_1(1 + R)/2 \tag{21}$$

for the extended time-delayed feedback. In Sections II C and II D we shall demonstrate how to derive other properties of the EDFC using the specific examples of chaotic systems, but first we consider general features of the EDFC for a simple example in which a linear approximation of the function $\phi(G)$ is assumed.

B. Properties of the EDFC: Simple example

To demonstrate the main properties of the EDFC let us suppose that the function $\phi(G)$ defining the FE for the proportional feedback depends linearly on the control gain G (cf. Refs. [38, 47]),

$$\phi(G) = \lambda_0(1 - G/G_1). \tag{22}$$

Here λ_0 denotes the dimensionless FE of the free system and G_1 is the stability threshold of the UPO controlled by proportional feedback. Substituting approximation (22) into Eq. (20) one derives the characteristic equation

$$k = (\lambda_0 - \lambda)\frac{1 + R\exp(-\lambda)}{1 + \exp(-\lambda)} \equiv \psi(\lambda) \tag{23}$$

defining the FEs for the EDFC. Here $k = K\lambda_0/G_1$ is the renormalized control gain of the extended time-delayed feedback. The periodic orbit is stable if all the roots of Eq. (23) are in the left half-plane $\mathrm{Re}\lambda < 0$. The characteristic root-locus diagrams and the dependence $\mathrm{Re}\lambda$ versus k for two different values of the parameter R are shown in Fig. 1. The zeros and poles of $\psi(\lambda)$ function define the value of roots at $k = 0$ and $k \to \infty$, respectively. For $k = 0$ (an open loop system), there is a real-valued root $\lambda = \lambda_0 > 0$ that corresponds to the FE of the free UPO and an infinite number of the complex roots $\lambda = \ln R + i\pi n$, $n = \pm 1, \pm 3, \ldots$ in the left half-plane associated with the extended delayed feedback controller. For $k \to \infty$, the roots tend to the locations $\lambda = i\pi n$, $n = \pm 1, \pm 3, \ldots$ determined by the poles of $\psi(\lambda)$ function. For intermediate values of K, the roots can evolve by two different scenario depending on the value of the parameter R.

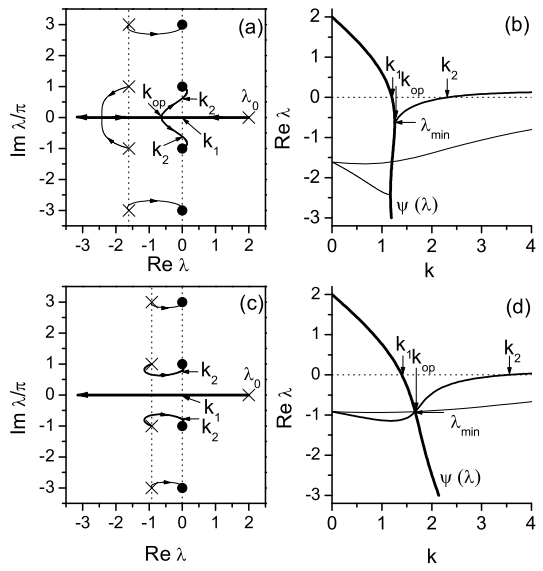

FIG. 1: Root loci of Eq. (23) as k varies from 0 to ∞ and dependence Reλ vs. k for $\lambda_0 = 2$ and two different values of the parameter R: (a) and (b) $R = 0.2 < R^\star$, (c) and (d) $R = 0.4 > R^\star$. The crosses and circles denote the location of roots at $k = 0$ and $k \to \infty$, respectively. Thick solid lines in (b) and (c) symbolized by $\psi(\lambda)$ are the dependencies $k = \psi(\lambda)$ for real λ.

If R is small enough ($R < R^\star$) the conjugate pair of the controller's roots $\lambda = \ln R \pm i\pi$ collide on the real axes [Fig. 1(a)]. After collision one of these roots moves along the real axes towards $-\infty$, and another approaches the FE of the UPO, then collides with this FE at $k = k_{op}$ and pass to the complex plane. Afterwards this pair of complex conjugate roots move towards the points $\pm i\pi$. At $k = k_2$ they cross into the right half-plane. In the interval $k_1 < k < k_2$ all roots of Eq. (23) are in the left half-plane and the UPO controlled by the extended time-delayed feedback is stable. The left boundary of the stability domain satisfies Eq. (21). For the renormalized value of the control gain it reads

$$k_1 = \lambda_0(1 + R)/2. \tag{24}$$

An explicit analytical expression for the right boundary k_2 is unavailable. Inside the stability domain there is an optimal value of the control gain $k = k_{op}$ that for the fixed R provides the minimal value λ_{min} for the real part of the leading FE [Fig. 1(b)]. To obtain the values k_{op} and λ_{min} it suffices to examine the properties of the function $\psi(\lambda)$ for the real values of the argument λ. The values k_{op} and λ_{min} are conditioned by the maximum of this function

and satisfy the equalities

$$\psi'(\lambda_{min}) = 0, \quad k_{op} = \psi(\lambda_{min}). \tag{25}$$

The above scenario is valid when the function $\psi(\lambda)$ possesses the maximum. The maximum disappears at $R = R^\star$, when it collides with the minimum of this function so that the conditions $\psi'(\lambda) = 0$ and $\psi''(\lambda) = 0$ are fulfilled. For $\lambda_0 = 2$, these conditions yield $R^\star \approx 0.255$.

Now we consider an evolution of roots for $R > R^\star$ [Fig. 1(c),(d)]. In this case the modes related to the controller and the UPO evolve independently from each other. The FE of the UPO moves along the real axes towards $-\infty$ without hibridizating with the modes of the controller. As previously the left boundary k_1 of the stability domain is determined by Eq. (24). The right boundary k_2 is conditioned by the controller mode associated with the roots $\lambda = \ln R \pm i\pi$ at $k = 0$ that move towards $\lambda = \pm i\pi$ for $k \to \infty$. The optimal value k_{op} is defined by a simple intersection of the real part of this mode with the mode related to the UPO.

Stability domains of the periodic orbit in the plane of parameters (k, R) are shown in Fig. 2(a). The left boundary of this domain is the straight line defined by Eq. (24). The right boundary is determined by parametric equations

$$k_2 = \frac{\lambda_0^2 + s^2}{\lambda_0 + s\cot(s/2)}, \quad R = \frac{\lambda_0 - s\cot(s/2)}{\lambda_0 + s\cot(s/2)}. \tag{26}$$

with the parameter s varying in the interval $[0, \pi]$. As is seen from the figure the stability domain is smaller for the UPOs with a larger FE λ_0. Figure 2(b) shows the optimal properties of the EDFC, namely, the dependence λ_{min} versus R, where λ_{min} is the value of the leading Floquet mode evaluated at $k = k_{op}$. This dependence possesses a minimum at $R = R_{op} = R^\star$. Thus for any given λ_0 there exists an optimal value of the parameter $R = R_{op}$ that at $k = k_{op}$ provides the fastest convergence of nearby trajectories to the desired periodic orbit. For $R > R_{op}$, the performance of the EDFC is adversely affected with the increase of R since for R close to 1 the modes of the controller are damped out very slowly, $\mathrm{Re}\lambda = \ln R$.

In this section we used an explicit analytical expression for the function $\phi(G)$ when analyzing the stability properties of the UPO controlled by the extended time-delayed feedback. In the next sections we consider a situation when the function $\phi(G)$ is available only numerically and only for real values of the parameter G. We show that in this case the main

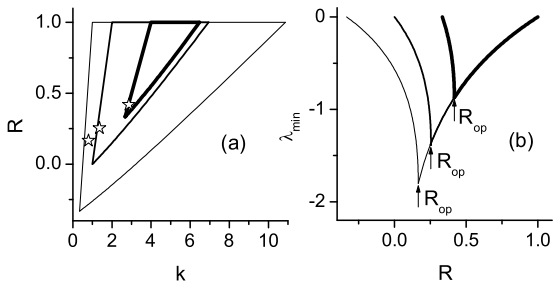

FIG. 2: (a) Stability domains of Eq. (23) in (k, R) plane and (b) dependence λ_{min} vs. R for different values of λ_0: 1, 2, and 4 (increasing line thickness corresponds to increasing values of λ_0). The stars inside the stability domains denote the optimal values (k_{op}, R_{op}).

stability characteristics of the system controlled by time-delayed feedback can be derived as well.

C. Rössler system

Let us consider the problem of stabilizing the period-one UPO of the Rössler system [49]:

$$\begin{pmatrix} \dot{x}_1 \\ \dot{x}_2 \\ \dot{x}_3 \end{pmatrix} = \begin{pmatrix} -x_2 - x_3 \\ x_1 + a x_2 \\ b + (x_1 - c) x_3 \end{pmatrix} + p(t) \begin{pmatrix} 0 \\ 1 \\ 0 \end{pmatrix}. \tag{27}$$

Here we suppose that the feedback perturbation $p(t)$ is applied only to the second equation of the Rössler system and the dynamic variable x_2 is an observable available at the system output, i.e., $y(t) = g\big(\boldsymbol{x}(t)\big) = x_2(t)$.

For parameter values $a = 0.2$, $b = 0.2$, and $c = 5.7$, the free ($p(t) \equiv 0$) Rössler system exhibits chaotic behavior. An approximate period of the period-one UPO $\boldsymbol{x}_0(t) = \boldsymbol{x}_0(t+T)$ embedded in chaotic attractor is $T \approx 5.88$. Linearizing Eq. (27) around the UPO one obtains explicit expressions for the matrices $A(t)$ and $B(t)$ defined in Eq. (8):

$$A(t) = \begin{pmatrix} 0 & -1 & -1 \\ 1 & a & 0 \\ x_3^0(t) & 0 & x_1^0(t) - c \end{pmatrix} \tag{28}$$

and $B = \mathrm{diag}(0, -1, 0)$. Here $x_j^0(t)$ denotes the j component of the UPO.

First we consider the system (27) controlled by proportional feedback, when the perturbation $p(t)$ is defined by Eq. (4). By solving Eqs. (10),(11) we obtain three FEs Λ_1, Λ_2 and Λ_3 as functions of the control gain G. The real parts of these functions are presented in Fig. 3(a). The values of the FEs of the free ($G = 0$) UPO are $\Lambda_1 T = 0.876 + i\pi$, $\Lambda_2 T = 0$, $\Lambda_3 T = -31.974 + i\pi$. Thus the first and the third FEs are located on the boundary of the "Brillouin zone." The second, zero FE, is related to the translational symmetry that is general for any autonomous systems. The dependence of the FEs on the control gain G is rather complex if it would be considered in a large interval of the parameter G. In Fig. 3(a), we restricted ourselves with a small interval of the parameter $G \in [0, 0.67]$ in which all FEs do not change their imaginary parts, e.i., the FEs Λ_1 and Λ_3 remain on the boundary of the "Brillouin zone," $\mathrm{Im}\Lambda_1 T = i\pi$, $\mathrm{Im}\Lambda_3 T = i\pi$ and Λ_2 remains real-valued, $\mathrm{Im}\Lambda_2 = 0$ for any G in the above interval. An information on the behavior of the leading FE Λ_1 or, more precisely, of the real-valued function $\phi(G) = \Lambda_1 T - i\pi$ in this interval will suffice to derive the main stability properties of the system controlled by time-delayed feedback.

The main information on the EDFC performance can be gained from parametric Eqs. (20). They make possible a simple reconstruction of the relevant Floquet branch in the (K, λ) plane. This Floquet branch is shown in Fig. 3(b) for different values of the parameter R. Let us denote the dependence K versus λ corresponding to this branch by a function ψ, $K = \psi(\lambda)$. Formally, an explicit expression for this function can be written in the form

$$\psi(\lambda) = \phi^{-1}(\lambda)\frac{1 + R\exp(-\lambda)}{1 + \exp(-\lambda)}, \tag{29}$$

where ϕ^{-1} denotes the inverse function of $\phi(G)$. More convenient for graphical representation of this dependence is, of course, the parametric form (20). The EDFC will be successful if the maximum of this function is located in the region $\lambda < 0$. Then the maximum defines the minimal value of the leading FE λ_{min} for the EDFC and $K_{op} = \psi(\lambda_{min})$ is the optimal value of the control gain at which the fastest convergence of the nearby trajectories to the desired orbit is attained. From Fig. 3(b) it is evident, that the delayed feedback controller should gain in performance through increase of the parameter R since the maximum of the $\psi(\lambda)$ function moves to the left. At $R = R^\star \approx 0.28$ the maximum disappears. For $R > R^\star$, it is difficult to predict the optimal characteristics of the EDFC. In Section II B we have established that in this case the value λ_{min} is determined by the intersection of different Flobquet branches.

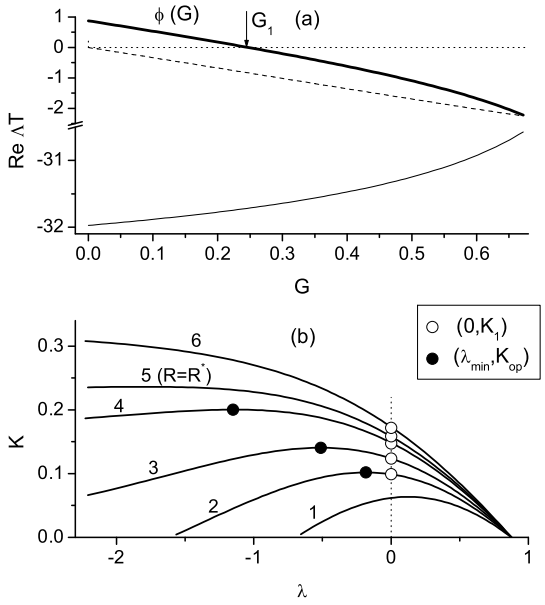

FIG. 3: (a) FEs of the Rösler system under PFC as functions of the control gain G. Thick solid, thin broken, and thin solid lines represent the functions $\Lambda_1 T - i\pi$, $\Lambda_2 T$ (zero exponent), and $\Lambda_3 T - i\pi$, respectively. (b) Parametric dependence K vs. λ defined by Eqs. (20) for the EDFC. The numbers mark the curves with different values of the parameter R: (1) -0.5, (2) -0.2, (3) 0, (4) 0.2, (5) 0.28, (6) 0.4. Solid dots show the maxima of the curves and open circles indicate their intersections with the line $\lambda = 0$.

The left boundary of the stability domain is defined by equality $K_1 = \psi(0)$ [Fig. 3(b)] or alternatively by Eq. (21), $K_1 = G_1(1 + R)/2$. This relationship between the stability thresholds of the periodic orbit controlled by the PFC and the EDFC is rather universal; it is valid for systems whose leading FE of the UPO is placed on the boundary of the "Brillouin zone." It is interesting to note that the stability threshold for the original DFC ($R = 0$) is equal to the half of the threshold in the case of the PFC, $K_1 = G_1/2$.

An evaluation of the right boundary K_2 of the stability domain is a more intricate problem. Nevertheless, for the parameter $R < R^\star$ it can be successfully solved by means of an analytical continuation of the function $\psi(\lambda)$ on the complex region. For this purpose we expend the function $\psi(\lambda)$ at the point $\lambda = \lambda_{min}$ into power series

$$\psi(\lambda) = K_{op} + \sum_{n=2}^{N+1} \alpha_n (\lambda - \lambda_{min})^n. \tag{30}$$

The coefficients α_n we evaluate numerically by the least-squares fitting. In this procedure we use a knowledge of numerical values of the function $\psi(\lambda_m)$, $m = 1, \ldots, M$ in $M > N$ points placed on the real axes and solve a corresponding system of N linear equations. To extend the Floquet branch to the region $K > K_{op}$ we have to solve the equation $K = \psi(\lambda)$ for the complex argument λ. Substituting $\lambda - \lambda_{min} = r\exp(i\varphi)$ into Eq. (30) we obtain

$$\sum_{n=2}^{N+1} \alpha_n r^n \sin n\varphi = 0, \tag{31a}$$

$$K = K_{op} + \sum_{n=2}^{N+1} \alpha_n r^n \cos n\varphi, \tag{31b}$$

$$\mathrm{Re}\lambda = \lambda_{min} + r\cos\varphi, \tag{31c}$$

$$\mathrm{Im}\lambda = r\sin\varphi. \tag{31d}$$

Let us suppose that r is an independent parameter. By solving Eq. (31a) we can determine φ as a function of r, $\varphi = \varphi(r)$. Then Eqs. (31b),(31c) and (31b),(31d) define the parametric dependencies $\mathrm{Re}\lambda$ versus K and $\mathrm{Im}\lambda$ versus K, respectively.

Figure 4 shows the dependence of the leading FEs on the control gain K for the EDFC. The thick solid line represents the most important Floquet branch that conditions the main stability properties of the system. It is described by the function $K = \psi(\lambda)$ with the real argument λ. Note that the same function has been depicted in Fig. 3(b) for inverted axes. For $R < R^\star$, this branch originates an additional sub-branch, which starts at the point (K_{op}, λ_{min}) and spreads to the region $K > K_{op}$. The sub-branch is described by Eqs. (31) that results from an analytical continuation of the function $\psi(\lambda)$ on the complex plane. This sub-branch is leading in the region $K > K_{op}$ and its intersections with the line $\lambda = 0$ defines the right boundary K_2 of the stability domain. In Figs. 4(a),(b) the sub-branches are shown by solid lines. As seen from the figures the Floquet sub-branches obtained by means of an analytical continuation are in good agreement with the "exact" solutions evaluated from the complete system of Eqs. (10),(15),(16).

For $R > R^\star$, the maximum in the function $\psi(\lambda)$ disappears and the Floquet branch originated from the eigenvalues $\lambda = \ln R \pm i\pi$ of the controller (see Section II B) becomes dominant in the region $K > K_{op}$. This Floquet branch as well as the intersection point (K_{op}, λ_{min}) are unpredictable via a simple analysis. It can be determined by solving the complete system of Eqs. (10),(15),(16). In Figs. 4(c),(d) these solutions are shown by dots.

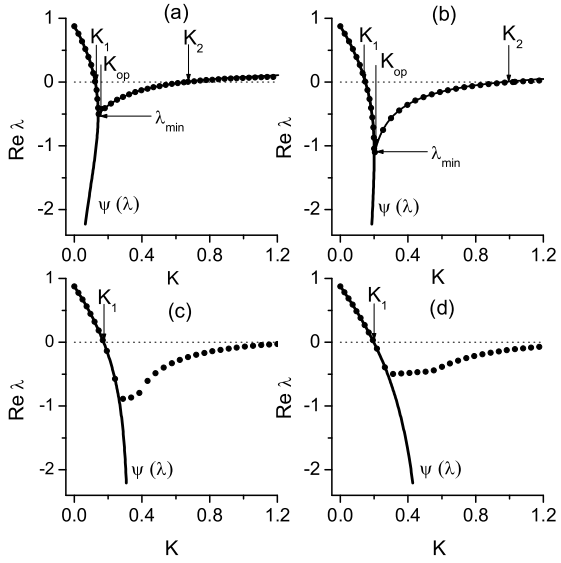

FIG. 4: Leading FEs of the Rösler system under EDFC as functions of the control gain K for different values of the parameter R: (a) 0.1, (b) 0.2, (c) 0.4, (d) 0.6. Thick solid lines symbolized by $\psi(\lambda)$ show the dependence $K = \psi(\lambda)$ for real λ. Solid lines in the region $K > K_{op}$ are defined from Eqs. (31). The number of terms in series (30) is N = 15. Solid black dots denote the "exact" solutions obtained from complete system of Eqs. (10),(15),(16).

Figure 5 demonstrates how much of information one can gain via a simple analysis of parametric Eqs. (20). These equations allows us to construct the stability domain in the (K, R) plane almost completely. The most important information on optimal properties of the EDFC can be obtained from these equations as well. The thick curve in the stability domain shows the dependence of optimal value of the control gain K_{op} on the parameter R. The star marks an optimal choice of both parameters (K_{op}, R_{op}), which provide the fastest decay of perturbations. Figure 5(b) shows how the decay rate λ_{min} attained at the optimal value of the control gain K_{op} depends on the parameter R. The left part of this dependence is simply defined by the maximum of the function $\psi(\lambda)$ while the right part is determined by intersection of different Floquet branches and can be evaluated only with the complete system of Eqs. (10),(15),(16). Unlike the simple model considered in Section II B here the intersection occurs before the maximum in the function $\psi(\lambda)$ disappears, i.e., at $R = R_{op} < R^{\star}$. Nevertheless, the value $R^{\star}$ gives a good estimate for the optimal value of

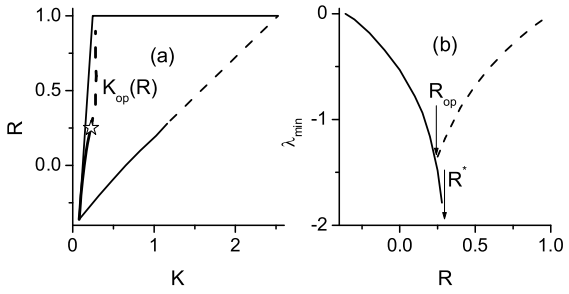

FIG. 5: (a) Stability domain of the period-one UPO of the Rössler system under EDFC. The thick curve inside the domain shows the dependence K_{op} versus R. The star marks the optimal point (K_{op}, R_{op}). (b) Minimal value λ_{min} of the leading FE as a function of the parameter R. In both figures solid and broken lines denote the solutions obtained from Eqs. (20) and Eqs. (10),(15),(16), respectively.

the parameter R, since $R^\star$ is close to R_{op}.

D. Duffing oscillator

To justify the universality of the proposed method we demonstrate its suitability for nonautonomous systems. As a typical example of such a system we consider the Duffing oscillator

$$\begin{pmatrix} \dot{x}_1 \\ \dot{x}_2 \end{pmatrix} = \begin{pmatrix} x_2 \\ x_1 - x_1^3 - \gamma x_2 + a\sin\omega t \end{pmatrix} + p(t) \begin{pmatrix} 0 \\ 1 \end{pmatrix}. \tag{32}$$

Here γ is the damping coefficient of the oscillator. The parameters a and ω are the amplitude and the frequency of the external force, respectively. We assume that the speed x_2 of the oscillator is the observable, i.e, $y(t) = g\big(\boldsymbol{x}(t)\big) = x_2$ and the feedback force $p(t)$ is applied to the second equation of the system (32). We fix the values of parameters $\gamma = 0.02$, $a = 2.5$, $\omega = 1$ so that the free ($p(t) \equiv 0$) system is in chaotic regime. The period of the period-one UPO embedded in chaotic attractor coincides with the period of the external force $T = 2\pi/\omega = 2\pi$. Linearization of Eq. (32) around the UPO yields the matrices $A(t)$ and $B(t)$ of the form

$$A(t) = \begin{pmatrix} 0 & 1 \\ 1 - 3\left[x_1^0(t)\right]^2 & -\gamma \end{pmatrix}, \quad B = \begin{pmatrix} 0 & 0 \\ 0 & -1 \end{pmatrix}. \tag{33}$$

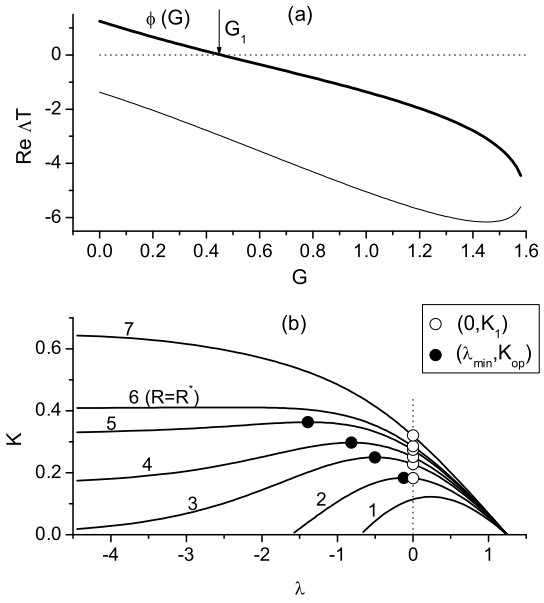

FIG. 6: (a) FEs of the Duffing oscillator under PFC as functions of the control gain G. Thick and thin solid lines denote the function $\Lambda_1 T - i\pi$ and $\Lambda_2 T - i\pi$, respectively. (b) The dependence K vs. λ for the EDFC defined by parametric Eqs. (20). The numbers mark the curves with different values of the parameter R: (1) -0.5, (2) -0.2, (3) 0, (4) 0.1, (5) 0.2, (6) 0.25, (7) 0.4

First we analyze the Duffing oscillator under proportional feedback defined by Eq. (4). This system is nonautonomous and does not have the zero FE. By solving Eqs. (10),(11) we obtain two FEs Λ_1 and Λ_2 as functions of the control gain G. The real parts of these functions are presented in Fig. 6(a). Both FEs of of the free ($G = 0$) UPO are located on the boundary of the "Brillouin zone," $\Lambda_1 T = 1.248 + i\pi$, $\Lambda_2 T = 0$, $\Lambda_2 T = -1.373 + i\pi$. As before, we restrict ourselves with a small interval of the parameter $G \in [0, 1.6]$ in which both FEs remain on the boundary.

As well as in previous example the main properties of the system controlled by time-delayed feedback can be obtained from parametric Eqs. (20). Fig. 6(b) shows the dependence $K = \psi(\lambda)$ for different values of the parameter R. For the fixed value of R, the maximum of this function defines the optimal control gain $K_{op} = \psi(\lambda_{min})$. The maximum disappears at $R = R^\star \approx 0.25$. The left boundary of the stability domain is $K_1 = \psi(0) = G_1(1 + R)/2$, as previously.

Figure 7 shows the results of analytical continuation of the relevant Floquet branch on

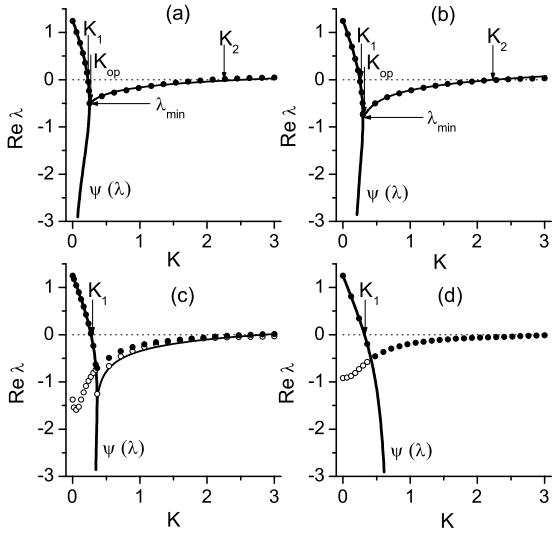

FIG. 7: The same as in Fig. 4 but for the Duffing oscillator. The values of the parameter R are: (a) 0., (b) 0.1, (c) 0.2, (d) 0.4. Open circles denote the second largest FE obtained from complete system of Eqs. (10),(15),(16).

the region $K > K_{op}$. The continuation is performed via Eqs. (31). For small values of the parameter R [Fig. 7(a),(b)], a good quantitative agreement with the "exact" result obtained from complete system of Eqs. (10),(15),(16) is attained. For $R = 0.2 < R^{\star}$, the Floquet mode associated with the controller becomes dominant in the region $K > K_{op}$. In this case the analytical continuation predicts correctly the second largest FE.

Again, as in previous example, a simple analysis of parametric Eqs. 20 allows us to construct the stability domain in the (K, R) plane almost completely [Fig. 8(a)] and to obtain the most important information on the optimal properties of the delayed feedback controller [Fig. 8(b)].

III. STABILIZING TORSION-FREE PERIODIC ORBITS

In Section II we restricted ourselves to the consideration of unstable periodic orbits erasing from a flip bifurcation. The leading Floquet multiplier of such orbits is real and negative (or corresponding FE lies on the boundary of the "Brillouin zone", $\mathrm{Im}\Lambda = \pi/T$). Such a consideration is motivated by the fact that the usual DFC and EDFC methods work only

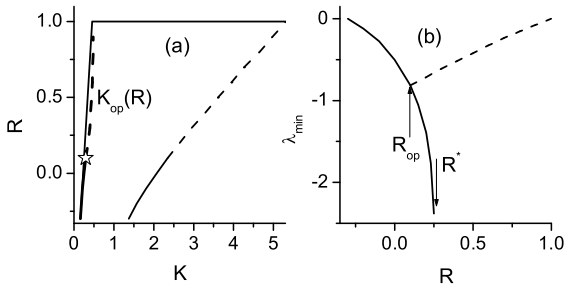

FIG. 8: The same as in Fig. 5 but for the Duffing oscillator.

for the orbits with a finite torsion, when the leading FE obeys $\mathrm{Im}\Lambda \neq 0$. Unsuitability of the DFC technique to stabilize torsion-free orbits ($\mathrm{Im}\Lambda = 0$) has been over several years considered as a main limitation of the method [37–40]. More precisely, the limitation is that any UPOs with an odd number of real Floquet multipliers greater than unity can never be stabilized by the DFC. This limitation can be explained by bifurcation theory as follows. When a UPO with an odd number of real FMs greater than unity is stabilized, one of such multipliers must cross the unite circle on the real axes in the complex plane. Such a situation correspond to a tangent bifurcation, which is accompanied with a coalescence of T-periodic orbits. However, this contradicts the fact that DFC perturbation does not change the location of T-periodic orbits when the feedback gain varies, because the feedback term vanishes for T-periodic orbits.

Here we describe an unstable delayed feedback controller that can overcome the limitation. The idea is to artificially enlarge a set of real multipliers greater than unity to an even number by introducing into a feedback loop an unstable degree of freedom.

A. Simple example: EDFC for $R > 1$

First we illustrate the idea for a simple unstable discrete time system $y_{n+1} = \mu_s y_n$, $\mu_s > 1$ controlled by the EDFC:

$$y_{n+1} = \mu_s y_n - K F_n, \tag{34}$$

$$F_n = y_n - y_{n-1} + R F_{n-1}. \tag{35}$$

The free system $y_{n+1} = \mu_s y_n$ has an unstable fixed point $y^\star = 0$ with the only real eigenvalue $\mu_s > 1$ and, in accordance with the above limitation, can not be stabilized by the EDFC for any values of the feedback gain K. This is so indeed if the EDFC is stable, i.e., if the parameter R in Eq. (35) satisfies the inequality $|R| < 1$. Only this case has been considered in the literature. However, it is easy to show that the unstable controller with the parameter $R > 1$ can stabilize this system. Using the ansatz $y_n, F_n \propto \mu^n$ one obtains the characteristic equation

$$(\mu - \mu_s)(\mu - R) + K(\mu - 1) = 0 \tag{36}$$

defining the eigenvalues μ of the closed loop system (34,35). The system is stable if both roots $\mu = \mu_{1,2}$ of Eq. (36) are inside the unit circle of the μ complex plain, $|\mu_{1,2}| < 1$. Figure 1 (a) shows the characteristic root-locus diagram for $R > 1$, as the parameter K varies from 0 to ∞. For $K = 0$, there are two real eigenvalues greater than unity, $\mu_1 = \mu_s$ and $\mu_2 = R$, which correspond to two independent subsystems (34) and (35), respectively; this means that both the controlled system and controller are unstable. With the increase of K, the eigenvalues approach each other on the real axes, then collide and pass to the complex plain. At $K = K_1 \equiv \mu_s R - 1$ they cross symmetrically the unite circle $|\mu| = 1$. Then both eigenvalues move inside this circle, collide again on the real axes and one of them leaves the circle at $K = K_2 \equiv (\mu_s + 1)(R + 1)/2$. In the interval $K_1 < K < K_2$, the closed loop system (34,35) is stable. By a proper choice of the parameters R and K one can stabilize the fixed point with an arbitrarily large eigenvalue μ_s. The corresponding stability domain is shown in Fig. 1 (b). For a given value μ_s, there is an optimal choice of the parameters $R = R_{op} \equiv \mu_s/(\mu_s - 1)$, $K = K_{op} \equiv \mu_s R_{op}$ leading to zero eigenvalues, $\mu_1 = \mu_2 = 0$, such that the system approaches the fixed point in finite time.

It seems attractive to apply the EDFC with the parameter $R > 1$ for continuous time systems. Unfortunately, this idea fails. As an illustration, let us consider a continuous time version of Eqs. (34,35)

$$\dot{y}(t) = \lambda_s y(t) - KF(t), \tag{37}$$

$$F(t) = y(t) - y(t - \tau) + RF(t - \tau), \tag{38}$$

where $\lambda_s > 0$ is the characteristic exponent of the free system $\dot{y} = \lambda_s y$ and τ is the delay time. By a suitable rescaling one can eliminate one of the parameters in Eqs. (37,38). Thus, without a loss of generality we can take $\tau = 1$. Equations (37,38) can be solved

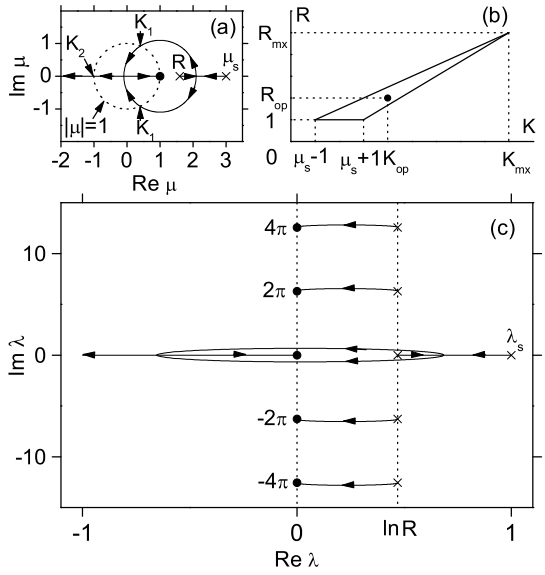

FIG. 9: Performance of (a,b) discrete and (c) continuous EDFC for $R > 1$. (a) Root loci of Eq. (36) at $\mu_s = 3$, $R = 1.6$ as K varies from 0 to ∞. (b) Stability domain of Eqs. (34,35) in the (K, R) plane; $K_{mx} = (\mu_s + 1)^2/(\mu_s - 1)$, $R_{mx} = (\mu_s + 3)/(\mu_s - 1)$. (c) Root loci of Eq. (39) at $\lambda_s = 1$, $R = 1.6$. The crosses and circles denote the location of roots at $K = 0$ and $K \to \infty$, respectively.

by the Laplace transform or simply by the substitution $y(t), F(t) \propto e^{\lambda t}$, that yields the characteristic equation:

$$1 + K \frac{1 - \exp(-\lambda)}{1 - R\exp(-\lambda)} \frac{1}{\lambda - \lambda_s} = 0. \tag{39}$$

In terms of the control theory, Eq. (39) defines the poles of the closed loop transfer function. The first and second fractions in Eq. (39) correspond to the EDFC and plant transfer functions, respectively. The closed loop system (37,38) is stable if all the roots of Eq. (39) are in the left half-plane, $\mathrm{Re}\lambda < 0$. The characteristic root-locus diagram for $R > 1$ is shown in Fig. 9 (c). When K varies from 0 to ∞, the EDFC roots move in the right half-plane from locations $\lambda = \ln R + 2\pi i n$ to $\lambda = 2\pi i n$ for $n = \pm 1, \pm 2 \ldots$. Thus, the continuous time EDFC with the parameter $R > 1$ has an infinite number of unstable degrees of freedom and many of them remain unstable in the closed loop system for any K.

B. Usual EDFC supplemented by an unstable degree of freedom

Hereafter, we use the usual EDFC at $0 \le R < 1$, however introduce an additional unstable degree of freedom into a feedback loop. More specifically, for a dynamical system $\dot{\boldsymbol{x}} = \boldsymbol{f}(\boldsymbol{x}, p)$ with a measurable scalar variable $y(t) = g(\boldsymbol{x}(t))$ and an UPO of period τ at $p = 0$, we propose to adjust an available system parameter p by a feedback signal $p(t) = KF_u(t)$ of the following form:

$$F_u(t) = F(t) + w(t), \tag{40}$$

$$\dot{w}(t) = \lambda_c^0 w(t) + (\lambda_c^0 - \lambda_c^\infty) F(t), \tag{41}$$

$$F(t) = y(t) - (1-R)\sum_{k=1}^{\infty} R^{k-1} y(t - k\tau), \tag{42}$$

where $F(t)$ is the usual EDFC described by Eq. (38) or equivalently by Eq. (42). Equation (41) defines an additional unstable degree of freedom with parameters $\lambda_c^0 > 0$ and $\lambda_c^\infty < 0$. We emphasize that whenever the stabilization is successful the variables $F(t)$ and $w(t)$ vanish, and thus vanishes the feedback force $F_u(t)$. We refer to the feedback law (40–42) as an unstable EDFC (UEDFC).

To get an insight into how the UEDFC works let us consider again the problem of stabilizing the fix point

$$\dot{y} = \lambda_s y - KF_u(t), \tag{43}$$

where $F_u(t)$ is defined by Eqs. (40–42) and $\lambda_s > 0$. Here as well as in a previous example we can take $\tau = 1$ without a loss of generality. Now the characteristic equation reads:

$$1 + KQ(\lambda) = 0, \tag{44}$$

$$Q(\lambda) \equiv \frac{\lambda - \lambda_c^\infty}{\lambda - \lambda_c^0} \frac{1 - \exp(-\lambda)}{1 - R\exp(-\lambda)} \frac{1}{\lambda - \lambda_s}. \tag{45}$$

The first fraction in Eq. (45) corresponds to the transfer function of an additional unstable degree of freedom. Root loci of Eq. (44) is shown in Fig. 10. The poles and zeros of Q-function define the value of roots at $K = 0$ and $K \to \infty$, respectively. Now at $K = 0$, the EDFC roots $\lambda = lnR + 2\pi in$, $n = 0, \pm 1, \ldots$ are in the left half-plane. The only root λ_c^0 associated with an additional unstable degree of freedom is in the right half-plane. That root and the root λ_s of the fix point collide on the real axes, pass to the complex plane and at $K = K_1$ cross into the left half-plane. For $K_1 < K < K_2$, all roots of Eq. (44)

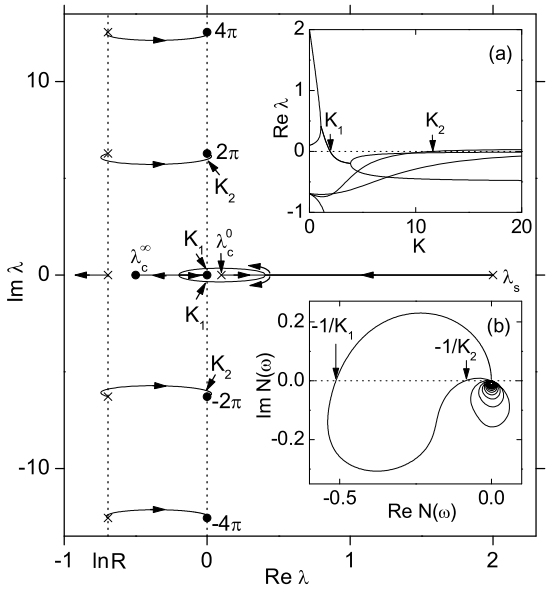

FIG. 10: Root loci of Eq. (44) at $\lambda_s = 2$, $\lambda_c^0 = 0.1$, $\lambda_c^\infty = -0.5$, $R = 0.5$. The insets (a) and (b) show Reλ vs. K and the Nyquist plot, respectively. The boundaries of the stability domain are $K_1 \approx 1.95$ and $K_2 \approx 11.6$.

satisfy the inequality Re$\lambda < 0$, and the closed loop system (40–43) is stable. The stability is destroyed at $K = K_2$ when the EDFC roots $\lambda = \ln R \pm 2\pi i$ in the second "Brillouin zone" cross into Re$\lambda > 0$. The dependence of the five largest Reλ on K is shown in the inset (a) of Fig. 10. The inset (b) shows the Nyquist plot, i.e., a parametric plot Re$N(\omega)$ versus Im$N(\omega)$ for $\omega \in [0, \infty]$, where $N(\omega) \equiv Q(i\omega)$. The Nyquist plot provides the simplest way of determining the stability domain; it crosses the real axes at Re$N = -1/K_1$ and Re$N = -1/K_2$.

As a more involved example let us consider the Lorenz system under the UEDFC:

$$\begin{pmatrix} \dot{x} \\ \dot{y} \\ \dot{z} \end{pmatrix} = \begin{pmatrix} -\sigma x + \sigma y \\ rx - y - xz \\ xy - bz \end{pmatrix} - KF_u(t) \begin{pmatrix} 0 \\ 1 \\ 0 \end{pmatrix}. \tag{46}$$

We assume that the output variable is y and the feedback force $F_u(t)$ [Eqs. (40–42)] perturbs only the second equation of the Lorenz system. Denote the variables of the Lorenz system by $\boldsymbol{\rho} = (x, y, z)$ and those extended with the controller variable w by $\boldsymbol{\xi} = (\boldsymbol{\rho}, w)^T$. For the parameters $\sigma = 10$, $r = 28$, and $b = 8/3$, the free ($K = 0$) Lorenz system has a period-

one UPO, $\boldsymbol{\rho}_0(t) \equiv (x_0, y_0, z_0) = \boldsymbol{\rho}_0(t+\tau)$, with the period $\tau \approx 1.5586$ and all real FMs: $\mu_1 \approx 4.714$, $\mu_2 = 1$ and $\mu_3 \approx 1.19 \times 10^{-10}$. This orbit can not be stabilized by usual DFC or EDFC, since only one FM is greater than unity. The ability of the UEDFC to stabilize this orbit can be verified by a linear analysis of Eqs. (46) and (40–42). Small deviations $\delta\boldsymbol{\xi} = \boldsymbol{\xi} - \boldsymbol{\xi}_0$ from the periodic solution $\boldsymbol{\xi}_0(t) \equiv (\boldsymbol{\rho}_0, 0)^T = \boldsymbol{\xi}_0(t+\tau)$ may be decomposed into eigenfunctions according to the Floquet theory, $\delta\boldsymbol{\xi} = e^{\lambda t}\boldsymbol{u}$, $\boldsymbol{u}(t) = \boldsymbol{u}(t+\tau)$, where λ is the Floquet exponent. The Floquet decomposition yields linear periodically time dependent equations $\delta\dot{\boldsymbol{\xi}} = A\delta\boldsymbol{\xi}$ with the boundary condition $\delta\boldsymbol{\xi}(\tau) = e^{\lambda\tau}\delta\boldsymbol{\xi}(0)$, where

$$A = \begin{pmatrix} -\sigma & \sigma & 0 & 0 \\ r - z_0(t) & -(1+KH) & -x_0(t) & -K \\ y_0(t) & x_0(t) & -b & 0 \\ 0 & (\lambda_c^0 - \lambda_c^\infty)H & 0 & \lambda_c^0 \end{pmatrix}. \tag{47}$$

Due to equality $\delta y(t - k\tau) = e^{-k\lambda\tau}\delta y(t)$, the delay terms in Eq. (42) are eliminated, and Eq. (42) is transformed to $\delta F(t) = H\delta y(t)$, where

$$H = H(\lambda) = (1 - exp(-\lambda\tau))/(1 - R\exp(-\lambda\tau)) \tag{48}$$

is the transfer function of the EDFC. The price for this simplification is that the Jacobian A, defining the exponents λ, depends on λ itself. The eigenvalue problem may be solved with an evolution matrix Φ_t that satisfies

$$\dot{\Phi}_t = A\Phi_t, \quad \Phi_0 = I. \tag{49}$$

The eigenvalues of Φ_τ define the desired exponents:

$$\det[\Phi_\tau(H) - e^{\lambda\tau} I] = 0. \tag{50}$$

We emphasize the dependence Φ_τ on H conditioned by the dependence of A on H. Thus by solving Eqs. (48–50), one can define the Floquet exponents λ (or multipliers $\mu = e^{\lambda\tau}$) of the Lorenz system under the UEDFC. Figure 11 (a) shows the dependence of the six largest Reλ on K. There is an interval $K_1 < K < K_2$, where the real parts of all exponents are negative. Basically, Fig. 11 (a) shows the results similar to those presented in Fig. 10 (a). The unstable exponent λ_1 of an UPO and the unstable eigenvalue λ_c^0 of the controller collide on the real axes and pass into the complex plane providing an UPO with a finite torsion.

Then this pair of complex conjugate exponents cross into domain $\mathrm{Re}\lambda < 0$, just as they do in the simple model of Eq. (43).

Direct integration of the nonlinear Eqs. (46, 40–42) confirms the results of linear analysis. Figures 11 (b,c) show a successful stabilization of the desired UPO with an asymptotically vanishing perturbation. In this analysis, we used a restricted perturbation similar as we did in Ref. [5]. For $|F(t)| < \varepsilon$, the control force $F_u(t)$ is calculated from Eqs. (40–42), however for $|F(t)| > \varepsilon$, the control is switched off, $F_u(t) = 0$, and the unstable variable w is dropped off by replacing Eq. (41) with the relaxation equation $\dot{w} = -\lambda_r w$, $\lambda_r > 0$.

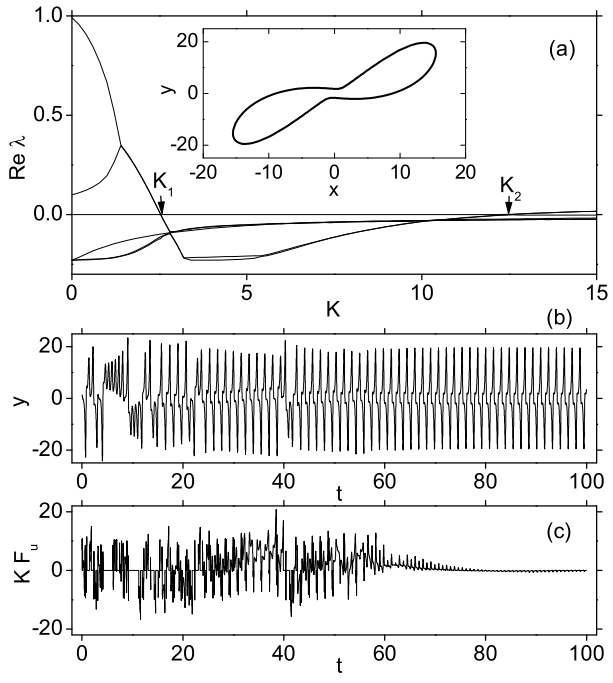

FIG. 11: Stabilizing an UPO of the Lorenz system. (a) Six largest $\mathrm{Re}\lambda$ vs. K. The boundaries of the stability domain are $K_1 \approx 2.54$ and $K_2 \approx 12.3$. The inset shows the (x, y) projection of the UPO. (b) and (c) shows the dynamics of $y(t)$ and $F_u(t)$ obtained from Eqs. (46,40–42). The parameters are: $\lambda_c^0 = 0.1$, $\lambda_c^\infty = -2$, $R = 0.7$, $K = 3.5$, $\varepsilon = 3$, $\lambda_r = 10$.

To verify the influence of fluctuations a small white noise with the spectral density $S(\omega) = a$ has been added to the r.h.s. of Eqs. (41,46). At every step of integration the variables x, y, z, and w were shifted by an amount $\sqrt{12ha}\xi_i$, where ξ_i are the random numbers uniformly distributed in the interval $[-0.5, 0.5]$ and h is the stepsize of integration. The control method

works when the noise is increased up to $a \approx 0.02$. The variance of perturbation increases proportionally to the noise amplitude, $\langle F_u^2(t) \rangle = ka$, $k \approx 17$. For a large noise $a > 0.02$, the system intermittently loses the desired orbit.

IV. STABILIZING AND TRACKING UNKNOWN STEADY STATES

Although the field of controlling chaos deals mainly with the stabilization of unstable periodic orbits, the problem of stabilizing unstable steady states of dynamical systems is of great importance for various technical applications. Stabilization of a fixed point by usual methods of classical control theory requires a knowledge of its location in the phase space. However, for many complex systems (e.g., chemical or biological) the location of the fixed points, as well as exact model equations, are unknown. In this case adaptive control techniques capable of automatically locating the unknown steady state are preferable. An adaptive stabilization of a fixed point can be attained with the time-delayed feedback method [5, 35, 50]. However, the use of time-delayed signals in this problem is not necessary and thus the difficulties related to an infinite dimensional phase space due to delay can be avoided. A simpler adaptive controller for stabilizing unknown steady states can be designed on a basis of ordinary differential equations (ODEs). The simplest example of such a controller utilizes a conventional low pass filter described by one ODE. The filtered dc output signal of the system estimates the location of the fixed point, so that the difference between the actual and filtered output signals can be used as a control signal. An efficiency of such a simple controller has been demonstrated for different experimental systems [50]. Further examples involve methods which do not require knowledge of the position of the steady state but result in a nonzero control signal [51].

In this section we describe a generalized adaptive controller characterized by a system of ODEs and prove that it has a topological limitation concerning an odd number of real positive eigenvalues of the steady state [44]. We show that the limitation can be overcome by implementing an unstable degree of freedom into a feedback loop. The feedback produces a robust method of stabilizing a priori unknown unstable steady states, saddles, foci, and nodes.

A. Simple example

An adaptive controller based on the conventional low-pass filter, successfully used in several experiments [50], is not universal. This can be illustrated with a simple model:

$$\dot{x} = \lambda^s(x - x^\star) + k(w - x), \quad \dot{w} = \lambda^c(w - x). \tag{51}$$

Here x is a scalar variable of an unstable one-dimensional dynamical system $\dot{x} = \lambda^s(x - x^\star)$, $\lambda^s > 0$ that we intend to stabilize. We imagine that the location of the fixed point $x^\star$ is unknown and use a feedback signal $k(w-x)$ for stabilization. The equation $\dot{w} = \lambda^c(w-x)$ for $\lambda^c < 0$ represents a conventional low-pass filter (rc circuit) with a time constant $\tau = -1/\lambda^c$. The fixed point of the closed loop system in the whole phase space of variables (x, w) is $(x^\star, x^\star)$ so that its projection on the x axes corresponds to the fixed point of the free system for any control gain k. If for some values of k the closed loop system is stable, the controller variable w converges to the steady state value $w^\star = x^\star$ and the feedback perturbation vanishes.

The closed loop system is stable if both eigenvalues of the characteristic equation $\lambda^2 - (\lambda^s + \lambda^c - k)\lambda + \lambda^s\lambda^c = 0$ are in the left half-plane $\mathrm{Re}\lambda < 0$. The stability conditions are: $k > \lambda^s + \lambda^c$, $\lambda^s\lambda^c > 0$. We see immediately that the stabilization is not possible with a conventional low-pass filter since for any $\lambda^s > 0$, $\lambda^c < 0$, we have $\lambda^s\lambda^c < 0$ and the second stability criterion is not met. However, the stabilization can be attained via an unstable controller with a positive parameter λ^c. Electronically, such a controller can be devised as the RC circuit with a negative resistance. Figure 12 shows a mechanism of stabilization. For $k = 0$, the eigenvalues are λ^s and λ^c, which correspond to the free system and free controller, respectively. With the increase of k, they approach each other on the real axes, then collide at $k = k_1$ and pass to the complex plane. At $k = k_0$ they cross symmetrically into the left half-plane (Hopf bifurcation). At $k = k_2$ we have again a collision on the real axes and then one of the roots moves towards $-\infty$ and another approaches the origin. For $k > k_0$, the closed loop system is stable. An optimal value of the control gain is k_2 since it provides the fastest convergence to the fixed point.

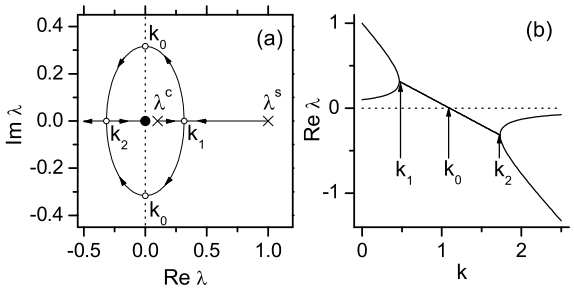

FIG. 12: Stabilizing an unstable fixed point with an unstable controller in a simple model of Eqs. (51) for $\lambda^s = 1$ and $\lambda^c = 0.1$. (a) Root loci of the characteristic equation as k varies from 0 to ∞. The crosses and solid dot denote the location of roots at $k = 0$ and $k \to \infty$, respectively. (b) Reλ vs. k. $k_0 = \lambda^s + \lambda^c$, $k_{1,2} = \lambda^s + \lambda^c \mp 2\sqrt{\lambda^s \lambda^c}$.

B. Generalized adaptive controller

Now we consider the problem of adaptive stabilization of a steady state in general. Let

$$\dot{\boldsymbol{x}} = \boldsymbol{f}(\boldsymbol{x}, \boldsymbol{p}) \tag{52}$$

be the dynamical system with N-dimensional vector variable $\boldsymbol{x}$ and and L-dimensional vector parameter $\boldsymbol{p}$ available for an external adjustment. Assume that an n-dimensional vector variable $\boldsymbol{y}(t) = \boldsymbol{g}\big(\boldsymbol{x}(t)\big)$ (a function of dynamical variables $\boldsymbol{x}(t)$) represents the system output. Suppose that at $\boldsymbol{p} = \boldsymbol{p}_0$ the system has an unstable fixed point $\boldsymbol{x}^\star$ that satisfies $\boldsymbol{f}(\boldsymbol{x}^\star, \boldsymbol{p}_0) = 0$. The location of the fixed point $\boldsymbol{x}^\star$ is unknown. To stabilize the fixed point we perturb the parameters by an adaptive feedback

$$\boldsymbol{p}(t) = \boldsymbol{p}_0 + kB[A\boldsymbol{w}(t) + C\boldsymbol{y}(t)] \tag{53}$$

where $\boldsymbol{w}$ is an M-dimensional dynamical variable of the controller that satisfies

$$\dot{\boldsymbol{w}}(t) = A\boldsymbol{w} + C\boldsymbol{y}. \tag{54}$$

Here A, B, and C are the matrices of dimensions $M \times M$, $M \times L$, and $n \times M$, respectively and k is a scalar parameter that defines the feedback gain. The feedback is constructed in such a way that it does not change the steady state solutions of the free system. For any k, the fixed point of the closed loop system in the whole phase space of variables $\{\boldsymbol{x}, \boldsymbol{w}\}$

is $\{\boldsymbol{x}^\star, \boldsymbol{w}^\star\}$, where $\boldsymbol{x}^\star$ is the fixed point of the free system and $\boldsymbol{w}^\star$ is the corresponding steady state value of the controller variable. The latter satisfies a system of linear equations $A\boldsymbol{w}^\star = -C\boldsymbol{g}(\boldsymbol{x}^\star)$ that has unique solution for any nonsingular matrix A. The feedback perturbation $kB\dot{\boldsymbol{w}}$ vanishes whenever the fixed point of the closed loop system is stabilized.

Small deviations $\delta\boldsymbol{x} = \boldsymbol{x} - \boldsymbol{x}^\star$ and $\delta\boldsymbol{w} = \boldsymbol{w} - \boldsymbol{w}^\star$ from the fixed point are described by variational equations

$$\delta\dot{\boldsymbol{x}} = J\delta\boldsymbol{x} + kPB\delta\dot{\boldsymbol{w}}, \quad \delta\dot{\boldsymbol{w}} = CG\delta\boldsymbol{x} + A\delta\boldsymbol{w}, \tag{55}$$

where $J = D_{\boldsymbol{x}}\boldsymbol{f}(\boldsymbol{x}^\star, \boldsymbol{p}_0)$, $P = D_{\boldsymbol{p}}\boldsymbol{f}(\boldsymbol{x}^\star, \boldsymbol{p}_0)$, and $G = D_{\boldsymbol{x}}\boldsymbol{g}(\boldsymbol{x}^\star)$. Here $D_{\boldsymbol{x}}$ and $D_{\boldsymbol{p}}$ denote the vector derivatives (Jacobian matrices) with respect to the variables $\boldsymbol{x}$ and parameters $\boldsymbol{p}$, respectively. The characteristic equation for the closed loop system reads:

$$\Delta_k(\lambda) \equiv \begin{vmatrix} I\lambda - J & -k\lambda PB \\ -CG & I\lambda - A \end{vmatrix} = 0. \tag{56}$$

For $k = 0$ we have $\Delta_0(\lambda) = |I\lambda - J||I\lambda - A|$ and Eq. (56) splits into two independent equations $|I\lambda - J| = 0$ and $|I\lambda - A| = 0$ that define N eigenvalues of the free system $\lambda = \lambda_j^s$, $j = 1, \ldots, N$ and M eigenvalues of the free controller $\lambda = \lambda_j^c$, $j = 1, \ldots, M$, respectively. By assumption, at least one eigenvalue of the free system is in the right half-plane. The closed loop system is stabilized in an interval of the control gain k for which all eigenvalues of Eq. (56) are in the left half-plane $\mathrm{Re}\lambda < 0$.

The following theorem defines an important topological limitation of the above adaptive controller. It is similar to the Nakajima theorem [39] concerning the limitation of the time-delayed feedback controller.

Theorem.—Consider a fixed point $\boldsymbol{x}^\star$ of a dynamical system (52) characterized by Jacobian matrix J and an adaptive controller (54) with a nonsingular matrix A. If the total number of real positive eigenvalues of the matrices J and A is odd, then the closed loop system described by Eqs. (52)-(54) cannot be stabilized by any choice of matrices A, B, C and control gain k.

Proof.—The stability of the closed loop system is determined by the roots of $\Delta_k(\lambda)$. Writing Eq. (56) for $k = 0$ in the basis where martcies J and A are diagonal, we have

$$\Delta_0(\lambda) = \prod_{j=1}^{N}(\lambda - \lambda_j^s)\prod_{m=1}^{M}(\lambda - \lambda_m^c). \tag{57}$$

Here λ_j^s and λ_m^c are the eigenvalues of the matrices J and A, respectively. Now from Eq. (56), we also have $\Delta_k(0) = \Delta_0(0)$, so Eq. (57) implies

$$\Delta_k(0) = \prod_{j=1}^{N}(-\lambda_j^s)\prod_{m=1}^{M}(-\lambda_m^c) \tag{58}$$

for all k. Since the total number of eigenvalues λ_j^s and λ_m^c that are real and positive is odd and other eigenvalues are real and negative or come in complex conjugate pairs, $\Delta_k(0)$ must be real and negative. On the other hand, from the definition of $\Delta_k(\lambda)$ we see immediately that when $\lambda \to \infty$ then $\Delta_k(\lambda) \to \lambda^{N+M} > 0$ for all k. $\Delta_k(\lambda)$ is an $N+M$ order polynomial with real coefficients and is continuous for all λ. Since $\Delta_k(\lambda)$ is negative for $\lambda = 0$ and is positive for large λ, it follows that $\Delta_k(\lambda) = 0$ for some real positive λ. Thus the closed loop system always has at least one real positive eigenvalue and cannot be stabilized, Q.E.D.

This limitation can be explained by bifurcation theory, similar to Ref. [39]. If a fixed point with an odd total number of real positive eigenvalues is stabilized, one of such eigenvalues must cross into the left half-plane on the real axes accompanied with a coalescence of fixed points. However, this contradicts the fact that the feedback perturbation does not change locations of fixed points.

From this theorem it follows that any fixed point $\boldsymbol{x}^\star$ with an odd number of real positive eigenvalues cannot be stabilized with a stable controller. In other words, if the Jacobian J of a fixed point has an odd number of real positive eigenvalues then it can be stabilized only with an unstable controller whose matrix A has an odd number (at least one) of real positive eigenvalues.

C. Controlling an electrochemical oscillator

The use of an unstable degree of freedom in a feedback loop is now demonstrated with control in an electrodissolution process, the dissolution of nickel in sulfuric acid. The main features of this process can be qualitatively described with a model proposed by Haim *et al.* [52]. The dimensionless model together with the controller reads:

$$\dot{e} = i - (1-\Theta)\left[\frac{C_h \exp(0.5e)}{1 + C_h \exp(e)} + a\exp(e)\right] \tag{59a}$$

$$\Gamma\dot{\Theta} = \frac{\exp(0.5e)(1-\Theta)}{1 + C_h\exp(e)} - \frac{bC_h\exp(2e)\Theta}{C_h c + \exp(e)} \tag{59b}$$

$$\dot{w} = \lambda^c(w - i) \tag{59c}$$

Here e is the dimensionless potential of the electrode and Θ is the surface coverage of NiO+NiOH. An observable is the current

$$i = (V_0 + \delta V - e)/R, \quad \delta V = k(i - w), \tag{60}$$

where V_0 is the circuit potential and R is the series resistance of the cell. δV is the feedback perturbation applied to the circuit potential, k is the feedback gain. From Eqs. (60) it follows that $i = (V_0 - e - kw)/(R - k)$ and $\delta V = k(V_0 - e - wR)/(R - k)$. We see that the feedback perturbation is singular at $k = R$.

In a certain interval of the circuit potential V_0, a free ($\delta V = 0$) system has three coexisting fixed points: a stable node, a saddle, and an unstable focus [Fig. 13(a)]. Depending on the initial conditions, the trajectories are attracted either to the stable node or to the stable limit cycle that surrounds an unstable focus. As is seen from Figs. 13(b) and 13(c) the coexisting saddle and the unstable focus can be stabilized with the unstable ($\lambda^c > 0$) and stable ($\lambda^c < 0$) controller, respectively if the control gain is in the interval $k_0 < k < R = 50$. Figure 13(d) shows the stability domains of these points in the (k, V_0) plane. If the value of the control gain is chosen close to $k = R$, the fixed points remain stable for all values of the potential V_0. This enables a tracking of the fixed points by fixing the control gain k and varying the potential V_0. In general a tracking algorithm requires a continuous updating of the target state and the control gain. Here described method finds the position of the steady states automatically. The method is robust enough in the examples investigated to operate without change in control gain. We also note that the stability of the saddle and focus points can be switched by a simple reversal of sign of the parameter λ^c.

Laboratory experiments for this system have been successfully carried out by I. Z. Kiss and J. L. Hudson [44]. They managed to stabilize and track both the unstable focus and the unstable saddle steady states. For the focus the usual rc circuit has been used, while the saddle point has been stabilized with the unstable controller. The robustness of the control algorithm allowed the stabilization of unstable steady states in a large parameter region. By mapping the stable and unstable phase objects the authors have visualized saddle-node and homoclinic bifurcations directly from experimental data.

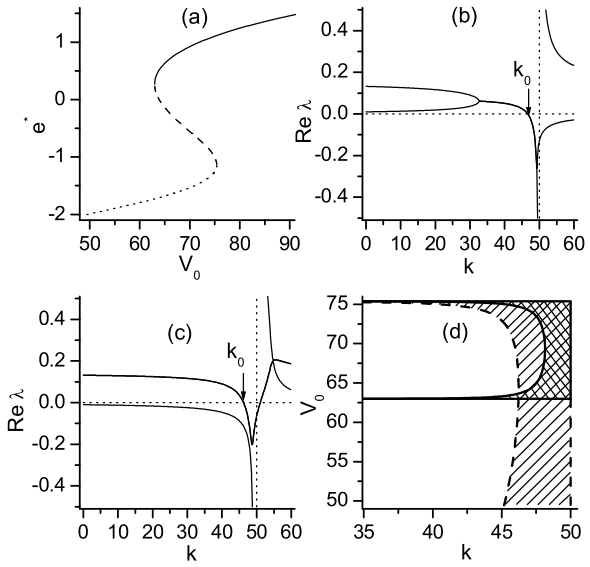

FIG. 13: Results of analysis of the electrochemical model for $R = 50$, $C_h = 1600$, $a = 0.3$, $b = 6 \times 10^{-5}$, $c = 10^{-3}$, $\Gamma = 0.01$. (a) Steady solutions $e^\star$ vs. V_0 of the free ($\delta V = 0$) system. Solid, broken, and dotted curves correspond to a stable node, a saddle, and an unstable focus, respectively. (b) and (c) Eigenvalues of the closed loop system as functions of control gain k at $V_0 = 63.888$ for the saddle $(e^\star, \Theta^\star) = (0, 0.0166)$ controlled by an unstable controller ($\lambda^c = 0.01$) and for the unstable focus $(e^\star, \Theta^\star) = (-1.7074, 0.4521)$ controlled by a stable controller ($\lambda^c = -0.01$), respectively. (d) Stability domain in (k, V_0) plane for the saddle (crossed lines) at $\lambda^c = 0.01$ and for the focus (inclined lines) at $\lambda^c = -0.01$.

V. CONCLUSIONS

The aim of this paper was to review experimental implementations, applications for theoretical models, and modifications of the time-delayed feedback control method and to present some recent theoretical ideas in this field.

In Section II, we have demonstrated how to utilize the relationship between the Floquet spectra of the system controlled by proportional and time-delayed feedback in order to obtain the main stability properties of the system controlled by time-delayed feedback. Our consideration has been restricted to low-dimensional systems whose unstable periodic orbits are originated from a period doubling bifurcation. These orbits flip their neighborhood during one turn so that the leading Floquet exponent is placed on the boundary of the

"Brillouin zone." Knowing the dependence of this exponent on the control gain for the proportional feedback control one can simply construct the relevant Floquet branch for the case of time-delayed feedback control. As a result the stability domain of the orbit controlled by time-delayed feedback as well as optimal properties of the delayed feedback controller can be evaluated without an explicit integration of time-delay equations. The proposed algorithm gives a better insight into how the Floquet spectrum of periodic orbits controlled by time-delayed feedback is formed. We believe that the ideas of this approach will be useful for further development of time-delayed feedback control techniques and will stimulate a search for other modifications of the method in order to gain better performance.

In Section III we discussed the main limitation of the delayed feedback control method, which states that the method cannot stabilize torsion-free periodic orbits, ore more precisely, orbits with an odd number of real positive Flocke exponents. We have shown that this topological limitation can be eliminated by introduction into a feedback loop an unstable degree of freedom that changes the total number of unstable torsion-free modes to an even number. An efficiency of the modified scheme has been demonstrated for the Lorenz system. Note that the stability analysis of the torsion-free orbits controlled by unstable controller can be performed in a similar manner as described in Section II. This problem is currently under investigation and the results will be published elsewhere.

In Section IV the idea of unstable controller has been used for the problem of stabilizing unknown steady states of dynamical systems. We have considered an adaptive controller described by a finite set of ordinary differential equations and proved that the steady state can never be stabilized if the system and controller in sum have an odd number of real positive eigenvalues. For two dimensional systems, this topological limitation states that only an unstable focus or node can be stabilized with a stable controller and stabilization of a saddle requires the presence of an unstable degree of freedom in a feedback loop. The use of the controller to stabilize and track saddle points (as well as unstable foci) has been demonstrated numerically with an electrochemical Ni dissolution system.

---

[1] R. Bellman, *Introduction to the Mathematical Theory of Control Processes* (Acad. Press, New York, 1971);

[2] G. Stephanopoulos, *Chemical Process Control: An Introduction to Theory and Practice* (Prentice-Hall, Englewood Cliffs, 1984);

[3] E. Ott, C. Grebogi, J. A. Yorke, Phys. Rev. Lett. **64**, 1196 (1990).

[4] T. Shinbrot, C. Grebogy, E. Ott, J. A. Yorke, Nature **363**, 411 (1993); T. Shinbrot, Advances in Phyzics **44**, 73 (1995); H. G. Shuster (Ed.) *Handbook of Chaos Control* (Willey-VCH, Weiheim, 1999); S. Boccaletti, C. Grebogi, Y.-C. Lai, H. Mancini, D. Maza, Physics Reports **329**, 103 (2000).

[5] K. Pyragas, Phys. Lett. A **170**, 421 (1992).

[6] K. Pyragas, A. Tamaševičius, Phys. Lett. A **180** 99 (1993); A. Kittel, J. Parisi, K. Pyragas, R. Richter, Z. Naturforsch. **49a** 843 (1994); D. J. Gauthier, D. W. Sukow, H. M. Concannon, J. E. S. Socolar, Phys. Rev. E **50**, 2343 (1994); P. Celka, Int. J. Bifurcation Chaos Appl. Sci. Eng. **4**, 1703 (1994).

[7] T. Hikihara, T. Kawagoshi, Phys. Lett. A **211**, 29 (1996); D. J. Christini, V. In, M. L. Spano, W. L. Ditto, J. J. Collins, Phys. Rev. E **56** R3749 (1997).

[8] S. Bielawski, D. Derozier, P. Glorieux, Phys. Rev. E **49**, R971 (1994); M. Basso, R. Genesio R, A. Tesi, Systems and Control Letters **31**, 287 (1997); W. Lu, D. Yu, R. G. Harrison, Int. J. Bifurcation Chaos Appl. Sci. Eng. **8**, 1769 (1998).

[9] T. Pierre, G. Bonhomme, A. Atipo, Phyz. Rev. Lett. **76** 2290 (1996); E. Gravier, X. Caron, G. Bonhomme, T. Pierre, J. L. Briancon, Europ. J. Phys. D **8**, 451 (2000).

[10] Th. Mausbach, Th. Klinger, A. Piel, A. Atipo, Th. Pierre, G. Bonhomme, Phys. Lett. A **228**, 373 (1997).

[11] T. Fukuyama, H. Shirahama, Y. Kawai, Physics of Plasmas **9**, 4525 (2002).

[12] O. Lüthje, S. Wolff, G. Pfister, Phys. Rev. Lett. **86**, 1745 (2001).

[13] P. Parmananda, R Madrigal, M. Rivera, L. Nyikos, I. Z. Kiss, V. Gaspar, Phys. Rev. E **59**, 5266 (1999); A. Guderian, A. F. Munster, M. Kraus, F. W. Schneider, J. of Phys. Chem. A **102**, 5059 (1998);

[14] H. Benner, W. Just, J. Korean Pysical Society **40**, 1046 (2002).

[15] J. M. Krodkiewski, J. S. Faragher, J. Sound and Vibration **234** (2000).

[16] K. Hall, D. J. Christini, M. Tremblay, J. J. Collins, L. Glass, J. Billette, Phys. Rev. Lett. **78**, 4518 (1997).

[17] C. Simmendinger, O. Hess, Phys. Lett. A **216**, 97 (1996).

[18] M. Munkel, F. Kaiser, O. Hess, Phys. Rev. E **56**, 3868 (1997); C. Simmendinger, M. Munkel, O. Hess, Chaos, Solitons and Fractals **10**, 851 (1999).

[19] W. J. Rappel, F. Fenton, A. Karma, Phys. Rev. Lett. **83**, 456 (1999).

[20] K. Konishi, H. Kokame, K. Hirata, Phyz. Rev. E **60**, 4000 (1999); K. Konishi, H. Kokame, K. Hirata, European Phyzical J. B **15**, 715 (2000).

[21] C. Batlle, E. Fossas, G. Olivar, Int. J. Circuit Theory and Applications **27**, 617 (1999).

[22] M. E. Bleich, J. E. S. Socolar, Int. J. Bifurcation Chaos Appl. Sci. Eng. **10**, 603 (2000).

[23] J. A. Holyst, K. Urbanowicz, Phsica A **287**, 587 (2000); J. A. Holyst, M. Zebrowska, K. Urbanowicz, European Phyzical J. B **20**, 531 (2001).

[24] A. P. M. Tsui, A. J. Jones, Physica D **135**, 135, 41 (2000).

[25] A. P. M. Tsui, A. J. Jones, Int. J. Bifurcation Chaos Appl. Sci. Eng. **9**, 713 (1999).

[26] P. Fronczak, J. A. Holyst, Phys. Rev. E **65**, 026219 (2002).

[27] B. Mensour, A. Longtin, Phys. Lett. A **205**, 18 (1995).

[28] U. Galvanetto, Int. J. Bifurcation Chaos Appl. Sci. Eng. **12**, 1877 (2002).

[29] K. Mitsubori, K. U. Aihara, Proceedings of the Royal Society of London Series A-Mathematical Phyzics and Engeneering Science **458**, 2801 (2002).

[30] K. Pyragas, Phys. Lett. A **198**, 433 (1995); H. Nakajima, H. Ito, Y. Ueda, IEICE Transactions on Fundamentals of Electronics Communications and Computer Sciencies, **E80A**, 1554, (1997); G. Herrmann, Phys. Lett. A **287**, 245 (2001).

[31] S. Boccaletti, F. T. Arecchi, Europhys. Lett. **31**, 127 (1995); S. Boccaletti, A. Farini, F. T. Arecchi, Chaos, Solitons and Fractals **8**, 1431 (1997).

[32] M. Basso, R. Genesio, A. Tesi, IEEE Trans. Circuits Syst. I **44**, 1023 (1997); M. Basso, R. Genesio, L Giovanardi, A. Tesi, G. Torrini, Int. J. Bifurcation Chaos Appl. Sci. Eng. **8**, 1699 (1998).

[33] M. E. Bleich, D. Hochheiser, J. V. Moloney, J. E. S. Socolar, Phys. Rev. E **55**, 2119 (1997); D. Hochheiser, J. V. Moloney, J. Lega, Phys. Rev. A **55**, R4011 (1997); N. Baba, A. Amann, E. Scholl, W. Just, Phys. Rev. Lett. **89**, 074101 (2002).

[34] J. E. S. Socolar, D. W. Sukow, D. J. Gauthier, Phys. Rev. E **50**, 3245 (1994).

[35] K. Pyragas, Phys. Lett. A **206**, 323 (1995).

[36] M. E. Bleich, J. E. S. Socolar, Phys. Lett. A **210**, 87 (1996).

[37] T. Ushio, IEEE Trans. Circuits Syst. I **43**, 815 (1996).

[38] W. Just, T. Bernard, M. Ostheimer, E. Reibold, H. Benner, Phys. Rev. Lett. **78**, 203 (1997).

[39] H. Nakajima, Phys. Lett. A **232**, 207 (1997).

[40] H. Nakajima, Y. Ueda, Physica D **111**, 143 (1998).

[41] S. Bielawsky, D. Derozier, P. Glorieux, Phys. Rev. A **47**, R2492 (1993); H.G. Shuster, M.B. Stemmler, Phys. Rev. E **56**, 6410 (1997).

[42] H. Nakajima, Y. Ueda, Phys. Rev. E **58**, 1757 (1998).

[43] K. Pyragas, Phys. Rev. Lett. **86**, 2265 (2001).

[44] K. Pyragas, V. Pyragas, I. Z. Kiss, J. L. Hudson, Phys. Rev. Lett. **89**, 244103 (2002).

[45] K. Pyragas, Phys. Rev. E **66**, 026207 (2002).

[46] G. Benettin, C. Froeschle, J. P. Scheidecker, Phys. Rev. A **19**, 2454 (1979); I. Schimada, T. Nagashima, Prog. Theor. Phys. **61**, 1605 (1979).

[47] W. Just, E. Reibold, H. Benner, K. Kacperski, P. Fronczak, J. Holyst, Phys. Lett. A **254**, 158 (1999); W. Just, E. Reibold, K. Kacperski, P. Fronczak, J. A. Holyst, H. Benner, Phys. Rev. E **61**, 5045 (2000).

[48] D. P. Lathrop, E. J. Kostelich, Phys. Rev. A **40**, 4028 (1989); P. So, E. Ott, S. J. Schiff, D. T. Kaplan, T. Sauer, C. Grebogi, Phys. Rev. Lett. **76**, 4705 (1996); P. So, E. Ott, T. Sauer, B. J. Gluckman, C. Grebogi, S. J. Schiff, Phys. Rev. E **55**, 5398 (1997).

[49] O. E. Rössler, Phys. Lett. A **57**, 397 (1976).

[50] A. Namajūnas, K. Pyragas, A. Tamaševičius, Phys. Lett. A **204**, 255 (1995); N. F. Rulkov, L. S. Tsimring, H. D. I. Abarbanel, Phys. Rev. E **50**, 314 (1994); A. S. Z. Schweinsberg, U. Dressler, Phys. Rev. E **63**, 056210 (2001).

[51] E. C. Zimmermann, M. Schell, J. Ross, J. Chem. Phys. **81**, 1327 (1984); J. Kramer, J. Ross, J. Chem. Phys. **83**, 6234 (1985); B. Macke, J. Zemmouri, N. E. Fettouhi, Phys. Rev. A **47**, R1609 (1993).

[52] D. Haim, O. Lev, L. M. Pismen, M. J. Sheintuch, J. Phys. Chem., **96**, 2676 (1992).